Journal of Glaciology

Article

Cite this article: Rowell IF, Mulvaney R, Rix J, Tetzner DR, Wolff EW (2022). Viability of chemical and water isotope ratio measurements of RAID ice chippings from Antarctica. *Journal of Glaciology* 1–16. https://doi.org/10.1017/jog.2022.94

Received: 23 March 2022
Revised: 17 August 2022
Accepted: 13 September 2022

Keywords:
Antarctic glaciology; ice core; ice coring; palaeoclimate; snow and ice chemistry

Author for correspondence:
Isobel F. Rowell, E-mail: ifr21@cam.ac.uk

© The Author(s), 2022. Published by Cambridge University Press on behalf of The International Glaciological Society. This is an Open Access article, distributed under the terms of the Creative Commons Attribution licence (http://creativecommons.org/licenses/by/4.0/), which permits unrestricted re-use, distribution and reproduction, provided the original article is properly cited.

cambridge.org/jog

Viability of chemical and water isotope ratio measurements of RAID ice chippings from Antarctica

Isobel F. Rowell[1], Robert Mulvaney[2], Julius Rix[2], Dieter R. Tetzner[1,2] and Eric W. Wolff[1]

[1]University of Cambridge, Cambridge, UK and [2]British Antarctic Survey, Cambridge, UK

Abstract

The British Antarctic Survey's (BAS) Rapid Access Isotope Drill (RAID), designed for rapid drilling to survey prospective ice core sites, has been deployed at multiple Antarctic locations over 6 years. This drilling method creates ice chippings that can be discretely sampled and analysed for their chemical and water isotopic composition. Ice sampling methods have evolved since the first uses of the BAS RAID, enabling a more quantifiable sample resolution. Here, we show that water isotope records obtained from RAID ice are comparable to those of equivalent depth resolution from proximal ice cores. Records of chemical impurities also show good agreement with nearby cores. Our findings suggest that the RAID is suitable for both chemical and isotopic reconnaissance of drilling sites. Residual contamination of certain ions is discussed, with proposed design changes to avoid this issue with future use.

Introduction

The British Antarctic Survey's (BAS) Rapid Access Isotope Drill (RAID) was designed to provide a high speed alternative to traditional ice core drilling methods, primarily in the polar regions. BAS's RAID is one of the several rapid drills proposed by groups involved with International Partnerships in Ice Core Sciences to address the need for high speed drilling (Wilhelms and others, 2006; Goodge and Severinghaus, 2016). Rapid drilling is useful for site surveying for large deep ice coring projects, such as Beyond EPICA: Oldest Ice (BE:OI) (Fischer and others, 2013; Parrenin and others, 2017). Rapid drilling techniques which allow either in situ measurements or collection of the ice for later analysis are highly advantageous. This is because preliminary measurements of the ice can be taken, including water isotope composition. Supplementing model and radar-based surveying, for example, these data provide further information about the site characteristics before undertaking a full-scale ice core drilling project which is time consuming and costly (Alemany and others, 2014; Schwander and others, 2014).

A detailed description of the drill engineering and design can be found in Rix and others (2019). In short, the RAID can drill to 600 m depth in up to 1.5 m increments, collecting ice chippings for sampling at the surface. Drilling to such a depth can be completed in ∼1 week. The single rotating barrel with external cutters and a fixed internal auger (Fig. 1) drills an 82.5 mm dry borehole which can be used for borehole measurements after drilling. While drilling, ice chippings rise up inside of the barrel. Once the barrel reaches the surface, the operator reverses the direction of the drill's rotation to empty the barrel. The ice chippings are then discretely sampled (Rix and others, 2019).

The drill has been successfully deployed at multiple locations around Antarctica. Test drilling at the BAS logistics base, Sky Blu, in the austral summer of 2015/16 was followed by two BE:OI site survey drillings at Little Dome C (LDC), East Antarctica in the austral summers of 2016/17 and 2017/18 (Passalacqua and others, 2018; Lilien and others, 2021). Most recently the drill has been used at Sherman Island, West Antarctica, in the austral summer of 2019/20 as part of the WACSWAIN (WArm Climate Stability of the West Antarctic in the last INterglacial) project (Rix and others, 2019; Mulvaney and others, 2021). The primary goal of WACSWAIN was to recover ice from the Last Interglacial (LIG) from a site on Skytrain Ice Rise, with a second drilling on Sherman Island to recover the longest possible record. The risk that viable LIG ice would not be found at the Sherman Island site was considered to be high for conventional ice core drilling. Therefore the RAID was used, with the intention of instead obtaining a lower resolution water isotope record from the site. This would indicate the ice age at the bedrock and give a first indication of the climate signal in the core. Using the RAID significantly reduces logistics, time and personnel expense, justifying fieldwork at the more high risk site (Mulvaney and others, 2021). For example, a comparison of BAS ice core drilling projects is provided in Table 2 of Mulvaney and others (2021) and shows that Sherman Island required only 25% of the total equipment mass of the next most lightweight drilling campaign, James Ross Island in 2007–08. The number of field personnel was less (five compared with six to eight, and could reasonably have been carried out with a three- or four-person team), and the field campaign was shorter at just 11 d in total, with 5 d of drilling. This

https://doi.org/10.1017/jog.2022.94 Published online by Cambridge University Press

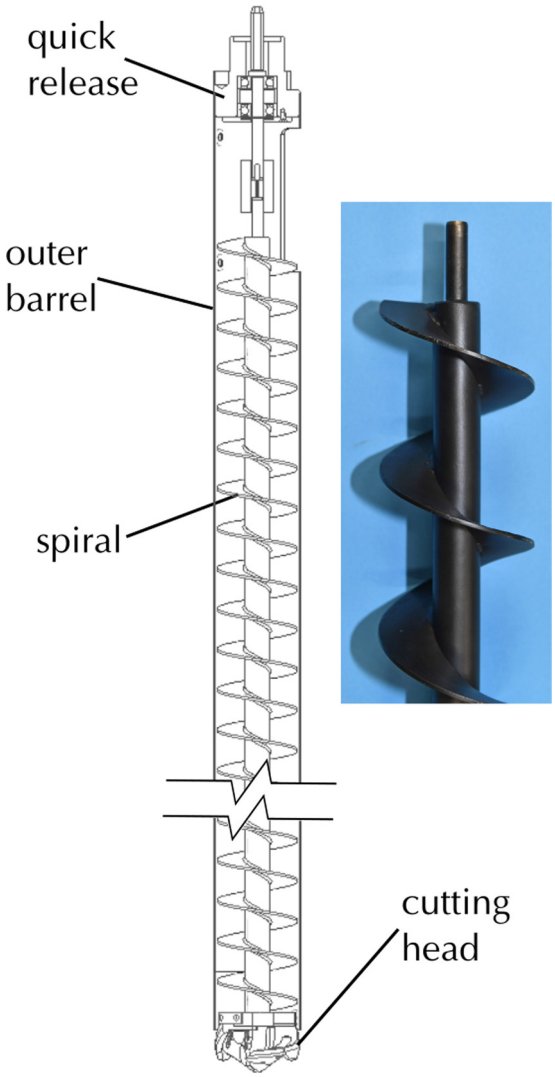

Fig. 1. RAID drill barrel and spiral (with the drill barrel shortened for clarity), showing the attachment mechanism at its top and cutter head at the bottom. From Rix and others (2019), Figure 4.

is due to much quicker average daily drilling progression, of 64.6 m d^{-1}, which is three to four times faster with the RAID compared to other BAS projects (Mulvaney and others, 2021).

Supplementing the available literature on the RAID and its use at LDC and Sherman Island, the focus here is on RAID ice sampling methods and the quality and validity of the lab-based ice measurements, specifically for stable water isotope and major ion chemistry. We use nearby ice cores to validate the RAID measurements, as described below.

Methods

Drill sites and sample collection

Drilling at LDC was the first attempt to use the RAID to recover ice for isotopic analysis, after Sky Blu drilling proved the RAID's technical capability. Two drilling campaigns were carried out: LDC 1 (named LDC:RAID1) and LDC 2. The RAID reached depths of 105 and 462 m during each of these campaigns, respectively (Rix and others, 2019). Here, we consider the longer record, which will be named LDC:RAID2. This nomenclature is based on the existing LDC:RAID1 site (Rix and others, 2019). We propose that future drilling sites in the LDC area, which is of intense interest for current and future drilling projects, be named similarly, specifying the project in the name where possible. Drilling at Sherman Island, located in the Abbott Ice Shelf to the south of Thurston Island on the coast of the WAIS, in the 2019/20 austral summer recovered samples to a depth of 323 m. The Sherman Island RAID ice (SI:RAID) borehole was drilled 2.7 km from a 20 m firn core (SI:Core) drilled on the island during the same field campaign (Tetzner and others, 2022). The LDC:RAID2 borehole site is 40.7 km from the EPICA Dome C (EDC) deep drilling site which we use for its comparison (EPICA community members, 2004). A map showing the respective locations of the study sites is shown in Figure 2 and a summary of the drilling campaigns is presented in Table 1.

The drilling and sampling process at LDC was the same at LDC-1 and LDC-2. The drill entered the borehole at the surface and was winched down to its last recorded depth. Rotation started and drilling into deeper ice began. When the full length of the barrel was filled with ice chippings, the drill rotation was stopped and the drill was winched out of the borehole. At the surface, the drill was rotated in reverse, allowing the ice chippings to pour out of the barrel. The operator would gradually move the emptying drill barrel along a sampling tray at an approximately constant speed so that the chippings were emptied in depth order along the tray. The tray was then visually divided into the number of samples needed for the required depth resolution based on the depth drilled during that drop (e.g. if 1.5 m had been drilled and a 15 cm depth resolution was desired, the tray would be split into ten even sections). The full depth range of each section was then sampled using a stainless steel scoop, as evenly as possible by eye, and the ice put into numbered zip-lock bags, sealed and transported frozen to the laboratory in Cambridge. The number and ID of samples from each drop were recorded. The subjective approach of sectioning the ice chippings in the sampling tray by eye presented room for improvement, by making the sampling resolution more quantifiable. Changes were subsequently made for the Sherman Island field campaign, described below.

At Sherman Island, the drilling protocol was carried out as at LDC, but when the drill returned to the surface, the drill was held statically over a funnel which directed the ice chippings into a long tube (1, 2, 3 in Fig. 3). The contents of the tube, from lowest depth to its top, are therefore in the same depth order as the ice inside the barrel and inside the ice sheet. The shallowest ice is at the top and the deepest at the bottom. The sampling tube (shown in Figs 3 and 4) has 5 cm windows at regular intervals. Stacked, rotate-able perspex rings (2 and 5, Fig. 3) encompassing the tube allow the windows to be open or closed. The windows were all placed in the closed position as the tube was filled with chippings (3, Fig. 3). As at LDC, using the known depth of the drop and the desired sampling resolution, the required number of samples was calculated. The correct number of windows required for one sample were then opened in sequence, starting at the top of the tube. Ice from the full depth range of each window was sampled evenly and the chippings scooped into numbered Whirl-Pak bags and stored in polystyrene ice core boxes for transport frozen to the laboratory. The number and ID of samples from each drop were recorded. Opening a fixed number of evenly sized windows makes this sampling method more objective, allowing a definitive depth range for each sample and reducing the potential for human error.

On occasion, the drill would bore deeper into the ice sheet than the average depth of drop. This would result in ice chippings spilling over into the sampling tube funnel. Initially, a sample was then taken from the chippings back-logged into the funnel. As drilling progressed, the decision was made to compact the chippings down into the tube before sampling using the window technique. The chippings were gently compacted by lifting and dropping the tube against the ground. With the sampling tube

https://doi.org/10.1017/jog.2022.94 Published online by Cambridge University Press

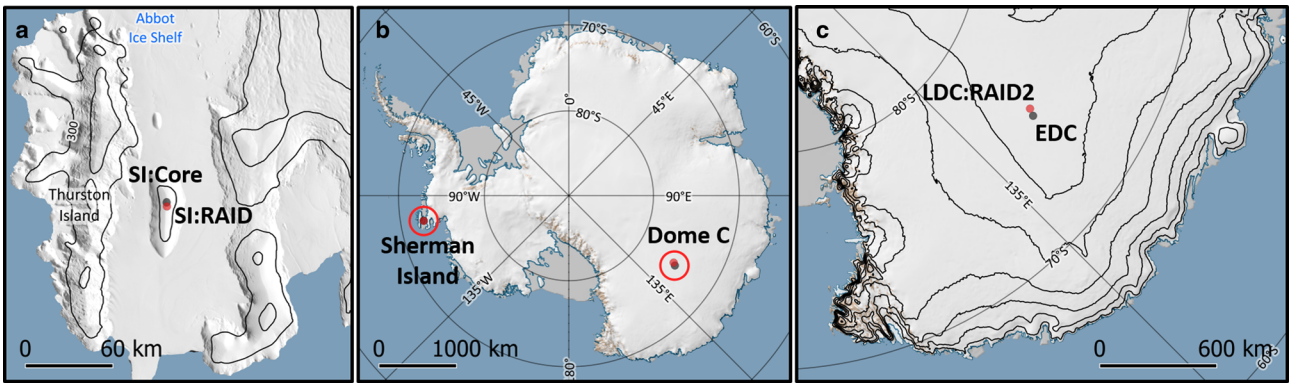

Fig. 2. Drilling locations used in this study. Red dots are RAID sites, grey dots are comparison cores. Sherman Island (panel A), showing 500 m elevation contours from CryoSat-2 and a MODIS Mosaic of Antarctica map projection to highlight the ridge line on Sherman Island. Dome C (panel C) showing 500 m elevation contours from CryoSat-2. Full map of Antarctica (panel B) with Sherman Island and Dome C areas circled in red, showing 1000 m elevation contours from the SCAR Antarctic Digital Database. Maps generated using QGIS with the Quantarctica mapping environment (Matsuoka and others, 2021).

filled with chippings, it was weighed after each drop (4, Fig. 3). By 180 m depth, the weight of the tube and chippings after each drop was consistent. This result indicated that maximum ice density (917 kg m^{-3}) had been reached, at which point weighing of the tube was stopped.

Sample preparation

Sample bags were removed from freezer ($<-20°C$) storage and spread out in trays in a class 100 clean laboratory to melt at room temperature. The melted sample was poured into an IC vial and a 1 mL aliquot was taken for the isotope sample. The IC samples were analysed and the isotope samples were boxed and refrigerated awaiting analysis at a later date.

Ion chromatography

Two Thermo Scientific Dionex Integrion High Pressure Ion Chromatography systems with conductivity detection were used to measure anions and cations. The anions measured were fluoride (F^-), chloride (Cl^-), sulphate (SO_4^{2-}), nitrate (NO_3^-) and methanesulphonate (MSA^-). Samples of 250 µL were separated into their constituent components using an AS17-C 250 mm analytical column and AG17-C 50 mm guard column, with 40 mM KOH eluent at a flow rate of 0.29 mL min^{-1}, before total conductivity detection, with use of a Dionex ADRS 600 (2 mm) suppressor. The cations measured were sodium (Na^+), ammonium (NH_4^+), potassium (K^+), magnesium (Mg^{2+}) and calcium (Ca^{2+}). Samples were separated using a CS16-4 µm 250 mm analytical column and CG16-4 µm 50 mm guard column, with 32 mM MSA eluent at a flow rate of 0.2 mL min^{-1}, before total conductivity detection, with use of a Dionex CDRS 600 (2 mm) suppressor.

Sample bags and blanks

The RAID was not originally intended to provide samples for IC measurement, so the cleanliness of the sampling method and tools and their suitability for such measurements was uncertain. The LDC:RAID2 samples were measured prior to the Sherman Island drilling season to determine if any method changes would be required. Blank analysis of the sample bags for both drilling campaigns was performed. Bags (Zip-lock, ZL, bags from the LDC campaign and Whirl-Pak, WP, for Sherman Island) were filled with ultra-pure Milli-Q (MQ) water and left at either room temperature in the clean lab, 2–5°C in the clean lab fridge or −18°C in the clean room freezer, for either 24 or 72 h. Thirty-two WP bags and 16 ZL bags (one from each box supplied) were prepared for each storage category. Bag blanks were prepared and analysed according to the standard protocols described above.

Calibration and blanks

Both instruments were calibrated weekly. Up to ten concentration levels of anion standards were used, and seven levels of cation standards covering the range of concentrations expected in the samples. During each measurement run, 2–4 of the calibration standards were loaded as check standards to monitor the ongoing performance of the instrument. Between 10 and 20 samples were loaded between each standard. During each calibration run and measurement run, European Reference Material (ERM) standards were also loaded and checked against their expected values. A minimum of two blanks (vials containing MQ water) were included at both the start and end of each sample sequence and periodically within the sequence.

Data processing

Instrument control and IC data processing were performed using Chromeleon Chromatography Data System (CDS) software, version 7. Data were exported and any erroneous results (e.g. injection errors) were then removed. Values that were below the detection limit were left in the data unaltered for initial investigation, as explained in the relevant results sections

Table 1. Summary of the RAID field campaigns at LDC and Sherman Island, with information about comparison core drilling projects EDC and SI:Core

	Latitude	Longitude	Elevation	Season	Depth	No. of samples	Resolution	Drilling time
Site	°	°	m		m		mean, cm	
LDC2	−75.36	122.42	3233	2017/18	461.58	1712	27.0	104.1
SI:RAID	−72.67	−99.71	440	2019/20	323.23	1724	18.8	45
EDC	−75.06	123.21	3233	1996–2004	3260	2123	5	N/A
SI:Core	−72.67	−99.63	440	2019/20	21.25	425	5	6

For EDC, the number of samples used is given as the IC measurements used for comparison, not the number of samples in the full dataset (there are multiple datasets).

https://doi.org/10.1017/jog.2022.94 Published online by Cambridge University Press

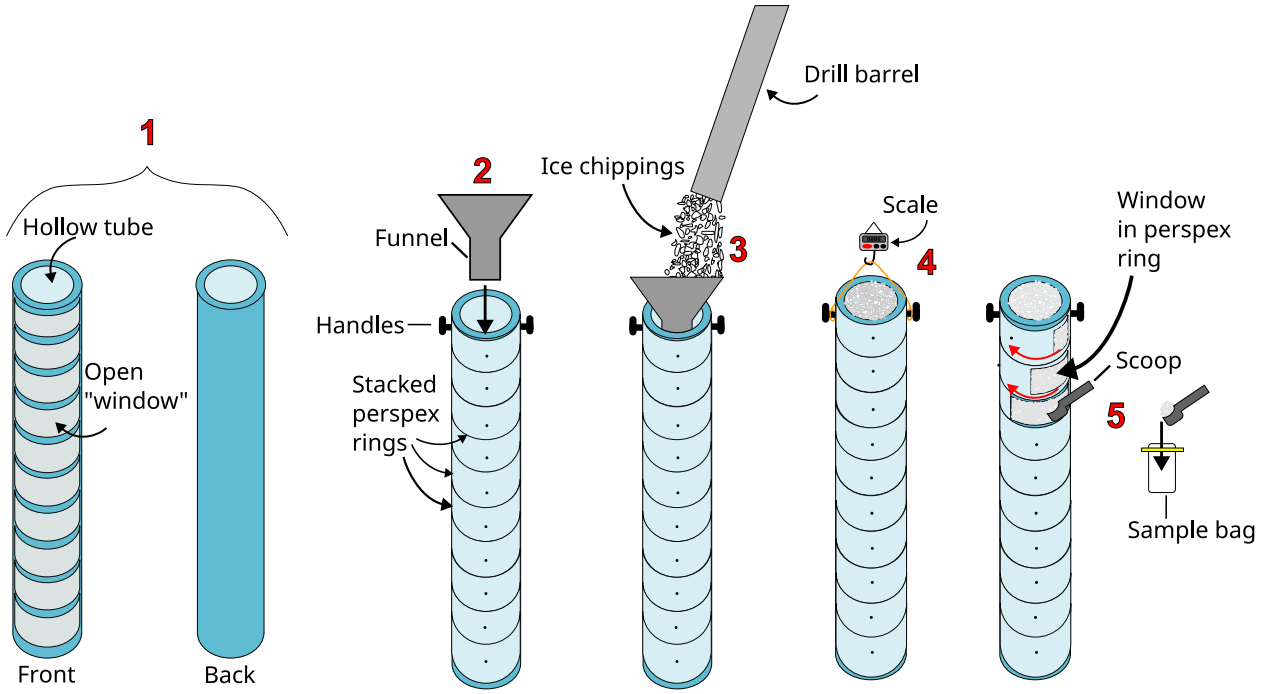

Fig. 3. Schematic diagram of the sampling tube and the sampling process for the SI:RAID samples.

below. For all analysis beyond Figure 9, sample concentrations below the detection limit were changed to the value of the detection limit for that species. For samples which produced very small chromatogram peaks not automatically detected using software detection parameters, manual integration of the peak was attempted; if the manually resolved peak returned a concentration of N/A, the concentration for that species was reported as N/A and not included in the statistics calculations. Fluoride peaks were difficult to separate and resolve due to interference in the chromatogram from organic species with similar retention times. Ammonium was difficult to calibrate at the lower concentrations required for the range of concentrations in samples. F^- and NH_4^+ data were subsequently removed from the datasets and any further analysis.

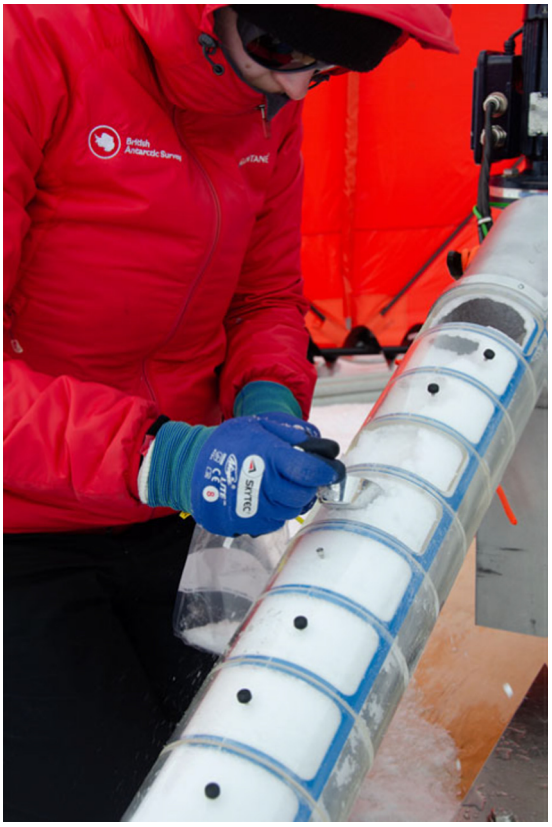

Fig. 4. BAS RAID sampling tube in use at Sherman Island.

Picarro cavity ring down spectrometry

Instrumentation

Stable water isotope ($\delta^{18}O$ and δ^2H) ratios were measured using a Picarro Cavity Ringdown Spectrometer (model L2130-i). One millilitre samples or 120 μL of standards were prepared. Between 2.2 to 3 μL of each sample were injected, to maintain an ideal minimum analysis water concentration of 18 000 parts per million. Samples were injected into the cavity through a 9.5 mm septum keeping the instrument cavity leak tight. The septum was replaced every run. The syringe was rinsed every run with solvent (1-methyl-2-pyrrolidinone) and replaced once per month. A standard 'high-throughput' method consisted of seven injections (measurements) of each sample, the data from the first three of which would be discarded to avoid carry-over effects from the residue of previous samples.

Calibration and standards

Standards were freshly prepared and loaded with each run of samples to calibrate the instrument, monitor ongoing performance and confirm that carry-over effects could be neglected. The external reference standard GRESP was regularly measured, in addition to multiple reference standards periodically throughout the LDC and SI analysis campaigns as performance checks, including for LDC the low value standard VSLAP. Statistics for δ^2H data from the standards most relevant for this study are shown in Table 2.

https://doi.org/10.1017/jog.2022.94 Published online by Cambridge University Press

Table 2. Summary statistics of the SI:RAID and LDC:RAID2 δ^2H and $\delta^{18}O$ data and standard deviations (SD, σ) from their respective analytical campaigns, showing sample data and external reference standards

	SI:RAID			LDC:RAID2			Standard values		
	Mean	σ injections	σ analysis	Mean	σ injections	σ analysis	Mean	σ injections	σ analysis
Sample δ^2H	−128.90	0.20	8.01	−403.15	0.2	22.59	N/A	N/A	N/A
GRESP δ^2H	−258.62	0.16	0.61	−258.1	0.29	0.89	−258.0	0.4	N/A
VSLAP-788 δ^2H	N/A	N/A	N/A	−429.38	0.16	0.32	−427.5	0.3	N/A
VSLAP-2453 δ^2H	N/A	N/A	N/A	−428.05	0.05	0.12	−427.5	0.3	N/A
Sample $\delta^{18}O$	−16.82	0.05	1.03	−50.69	0.07	2.66	N/A	N/A	N/A
GRESP $\delta^{18}O$	−33.39	0.03	0.12	−33.32	0.04	0.18	−33.4	0.04	N/A
VSLAP-788 $\delta^{18}O$	N/A	N/A	N/A	−55.50	0.03	0.04	−55.5	0.02	N/A
VSLAP-2453 $\delta^{18}O$	N/A	N/A	N/A	−55.23	0.01	0.02	−55.5	0.02	N/A

Mean is the final mean value across multiple injections for every analysis result. SD injections show the mean of the SD of injections 4–7 for each measured sample. SD analysis shows the SD for all sample data (all injections). 'SD analysis' is not provided by the manufacturers for the standards used.

Comparison data

Sherman Island

During the Sherman Island field campaign (January–February 2020), a 21.25 m firn core was also drilled 2.7 km away from the RAID drill site. The firn core was cut into 425 5 cm samples which were measured using ion chromatography and cavity ring down spectrometry at the BAS with the same methodology described in the methods section above (Tetzner and others, 2022). Available chemical (ions MSA^-, Cl^-, SO_4^{2-}, Na^+ and Ca^{2+}) and water isotope (δ^2H) data were used for assessing the data quality of equivalent measurements on the RAID samples. IC and water isotope measurements were obtained from all SI:RAID samples.

Dome C

Previously published chemistry data from the top 788 m of the EDC ice core were used for comparison with LDC:RAID2 (Littot and others, 2002). EDC analytical methods varied as the analysis was carried out by multiple lab groups, as described by Littot and others. Four sections of LDC:RAID2 samples were analysed for IC, from different depths. The four depth ranges correspond to four periods which we identify, in order of youngest to oldest, as Late Holocene, Early Holocene, ACR and Transition. The Dome C chemistry data were split into approximately the same age sections.

Publicly available water isotope data from the EDC ice core at 55 cm resolution ($\delta^{18}O$ and δ^2H) were used as a comparison for the LDC:RAID2 water isotope data (Stenni and others, 2010). Data from the EDC depths covering the same time period (~18 kyr at 462 m depth) as the LDC:RAID2 chippings are used for comparisons in this paper. All LDC:RAID2 samples were analysed for water isotope composition.

Focus

Both of the Sherman Island records (RAID and Core) were drilled from the surface of the island, and the sites are located <3 km apart. They both have measurements covering the full depth range of the top 21 m of the ice sheet on Sherman Island. At Dome C, the sites are over 40 km apart and only discrete sections, described above, of the LDC samples were analysed for IC measurements, so the exact overlap, in age terms, between the sections analysed at LDC is less clear. For these reasons, the results focus on more detail on interpretation of the Sherman Island data because we should expect more similarity between the Sherman Island records.

Results

Ion chromatography

Blank calculations

IC data detection limits from the Sherman Island analysis campaign are shown in Table 3. The limit of the blank was calculated according to Eqn (1):

$$\mathrm{LoB} = \mu_{\mathrm{blank}} + 1.645(\sigma_{\mathrm{blank}}), \quad (1)$$

where LoB is the highest concentration of analyte expected in a blank sample, the μ_{blank} is the mean of replicate measurements of ultra-pure MQ water and σ_{blank} is the standard deviation (SD, σ) of the blank (MQ) concentrations (Armbruster and Pry, 2008). The LoB was used here because the most dilute standard used has higher concentrations than typical blank values, positively skewing the LoD. In addition, the relative SDs of the blanks are low (0.35–1.42 depending on the species), showing that a consistent blank value is measured. The LoB is therefore used instead of the LoD.

Bags

The ion concentrations of MQ water stored in both WP and ZL bags is similar (within uncertainty) to that of normal procedural blank values, showing their suitability for use as non-contaminating containers for RAID samples. Supplementary Figure S1 shows the mean concentrations of all ionic species measured. Due to the negligible ($< 1\ \mu g\ L^{-1}$) concentrations of certain ions, a selection of the most concentrated ions (Cl^-, NO_3^-, SO_4^{2-} and Ca^{2+}) is discussed in more detail here with reference to Figure 5. With all of the concentrations below the limit of detection, meaningful comparison is limited. However the results in Figure 5 do confirm that the concentration of ions in the bags

Table 3. LoBs and percentages of measurements below LoB in the SI:RAID IC measurements, calculated using MQ blanks (n cations = 365, n anions = 390)

Analyte	SI LoB $\mu g\ L^{-1}$	SI below LoB %
Na^+	6.2	0
K^+	4.44	0.35
Mg^{2+}	4.98	0
Ca^{2+}	8.23	5.65
MSA^-	2.31	0.06
Cl^-	7.21	0
NO_3^-	8.99	0.93
SO_4^{2-}	8.59	0

For anions, sample $n = 1712$, for cations $n = 1698$.

https://doi.org/10.1017/jog.2022.94 Published online by Cambridge University Press

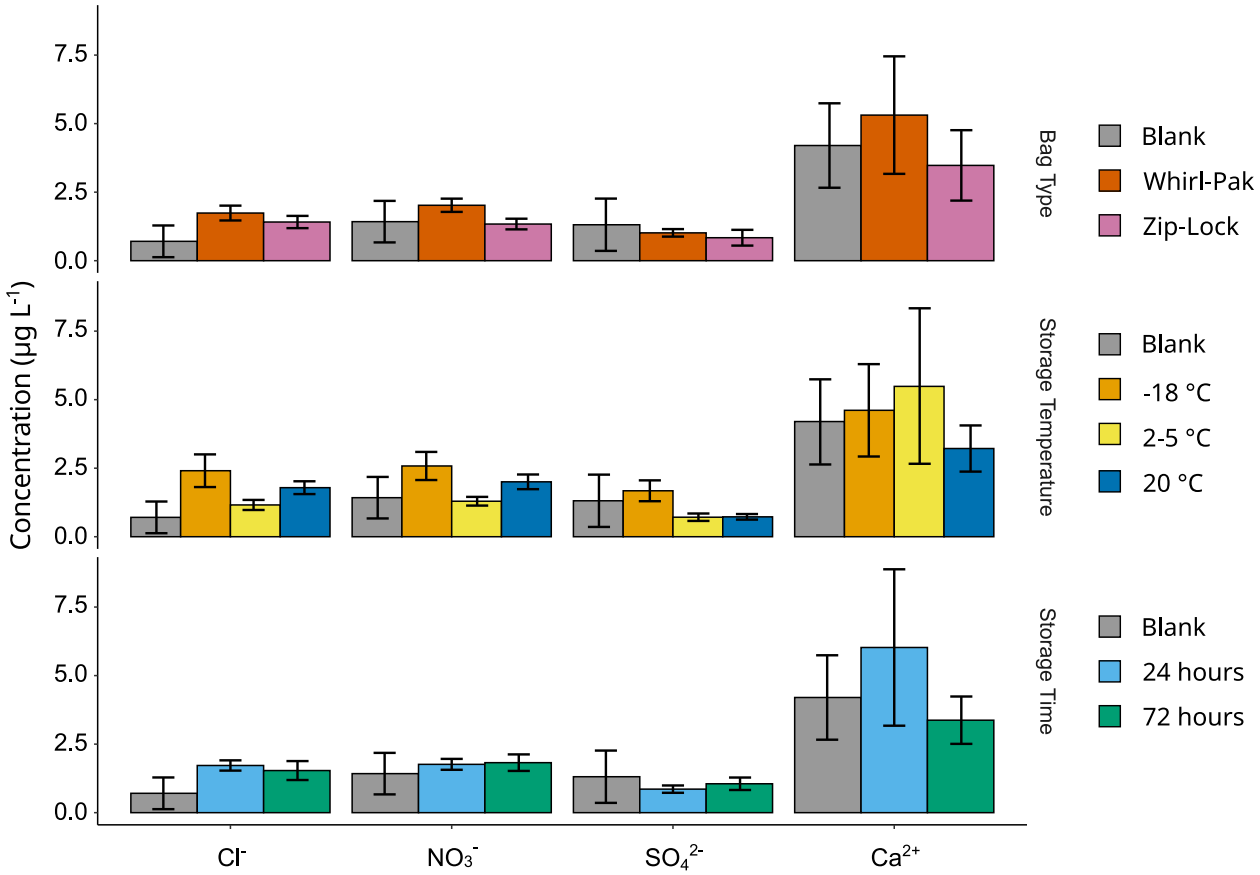

Fig. 5. Mean concentrations of selected ions in WP and ZL bags and blanks for comparison, plotted by bag type, storage time and location (colour legend). Note that all data are grouped then split by category. For example, the 24 h (light blue) bar includes data from both types of bags, stored at each temperature but only for 24 h; the Whirl-Pak (red) bar includes data from bags stored at each temperature and for all lengths of time, but only for Whirl-Pak bags, etc. For bag type $n = 32$ (WP) and $n = 16$ (ZL), for storage temperature $n = 12$ (lab and freezer) and $n = 24$ (fridge), for storage duration $n = 24$, for procedural blanks $n = 17$.

is comparable to that of the concentrations in procedural blanks run in the same analytical sequence. All bag mean concentrations including standard error (independent of bag type, storage time and location), are within the error of the procedural blank concentrations. The highest blank and test concentration is in Ca^{2+}. Both storage location and time have a negligible effect on contamination or potential leaching of chemicals in the plastic into the water. While all bag mean results for chloride are higher than for the blank, this is lower than the detection limit for this component (Table 3), and a large factor lower than any concentration in the chippings (e.g. Fig. 7). These results justify the use of either ZL or WP bag as RAID sample containers, with WP bags preferred due to being more user-friendly under cold conditions.

Contamination

The sample from the top of each drop of the drill is contaminated with artificially high ion concentrations, particularly with Ca^{2+} and K^{+}, as shown in Figure 6 and Table 4. A series of samples between 0.8 and 1.5 m depth (Fig. 6) with highly concentrated Ca^{2+} (four samples ranging from 160 to 308 µg L^{-1}) is not linked with sample position in the barrel drop. This could be a real feature because there is no corresponding increase in K^{+}. Alternatively, it is possible that a contaminant source in the shorter drill barrel which was present in the first two drops, was effectively washed out by the chippings. The SI:RAID data show that the systemic contamination problem is isolated to the longer (1.5 m) drill barrel, which was used from 11.6 m borehole depth. The periodic spikes, particularly in Ca^{2+}, are not visible above this depth. The shallowest LDC:RAID2 samples were not measured for chemistry so it is not known if this is also the case for the LDC samples, although the pattern of contamination in the available data is similar.

Figures 7, 8 and 9 show a good overview of contamination levels and demonstrate that contamination is restricted to the first sample in each drop, and is most prominent for Ca^{2+} and K^{+}. The SI:RAID data in Figure 7 also show higher means for some ions in positions eight and nine. However, the number of samples in both of these drop positions is much lower ($n = 10$ and 3 respectively). With such low sample sizes, it is not reasonable to conclude that there is contamination in these samples. The majority of drill drops contained seven samples and there is significant overlap and similarity in the box-plots of samples two to seven, indicating minimal contamination in all but the first sample.

Similarly in the LDC data, the overlap of box-plots of sample positions two to five convincingly shows that position one is the main sample affected by contamination. The positive skew in the LDC:RAID2 data seen in Figure 9 is due to the data extending back to 18 ka. The Late-Glacial Age samples have higher concentrations of all ions, as made clear by the age-coloured points.

Table 4 demonstrates that every ion shows an increase in the first drop, with Ca^{2+} showing a near 200% increase in the first sample, compared to only ~13% in NO_3^- and Cl^-. All of the mean differences are statistically significant in the results of a two-sample t test, with p values <0.05. However, the t statistic for K^{+} and Ca^{2+} is much higher. Similarly in Figure 8, K^{+} and Ca^{2+} are the only two species for which the upper limit of uncertainty (1 SD) on the mean concentration of samples 2–9 is lower than the mean concentration for sample 1. The Ca^{2+} and K^{+} data from the top sample of each drop were changed to the mean

https://doi.org/10.1017/jog.2022.94 Published online by Cambridge University Press

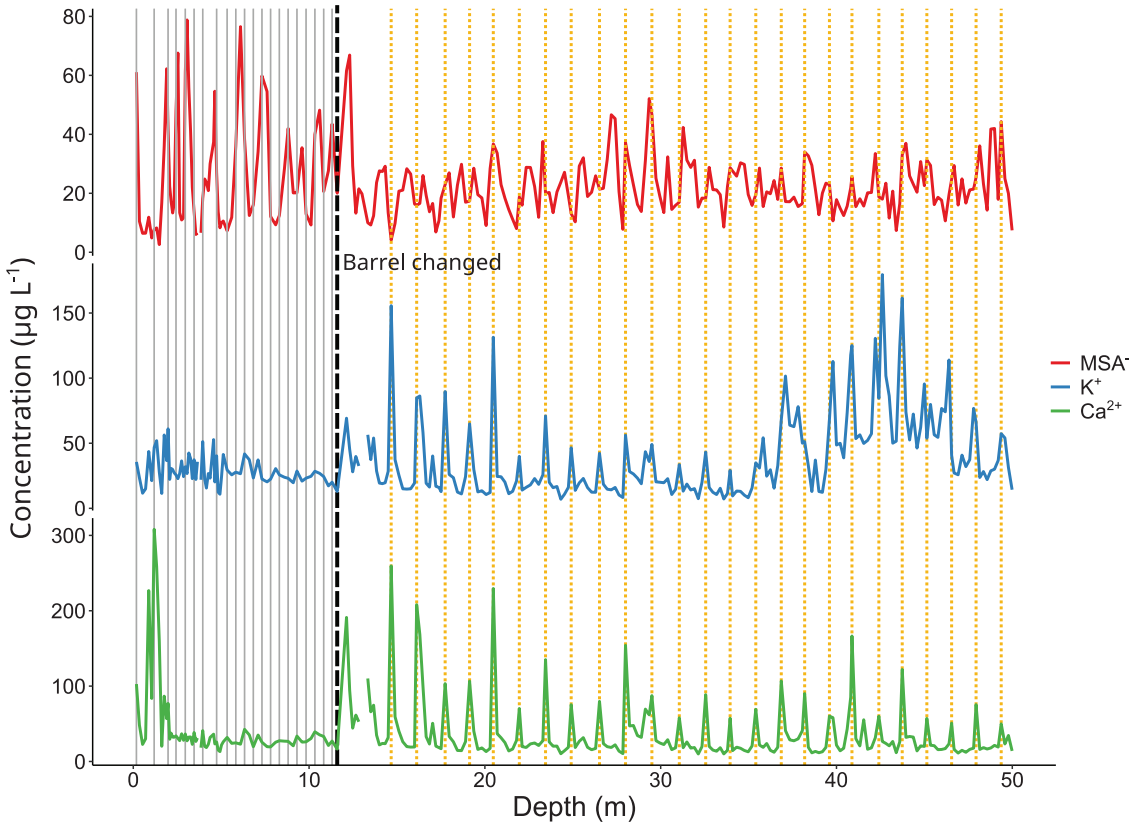

Fig. 6. Top 50 m of MSA, K and Ca in the Sherman Island RAID chippings. The dashed black line shows the depth at which the barrel was swapped from the shorter to longer barrel. Vertical dotted lines show the first sample of each drop before (grey) and after (orange) the barrel was changed.

value of the concentrations from the rest of the drop, for both sites' datasets, because they were deemed contaminated to an extent that rendered the data unusable.

Supplementary Figure S2 shows that the percentage difference between the first and remaining samples in the drop declines slightly with increasing depth in the SI:RAID borehole for some ions. If this decline were due to 'washing out' of the barrel with continuous flow of chippings, the most contaminated species (K^+ and Ca^{2+}) should show the greatest decline with depth. This is not the case, however, with the decreasing trend lines of K^+ and Ca^{2+} having r^2 values of 0.01 and 0.05 respectively. The greatest trend ($r^2 = 0.18$) is seen for NO_3^- which shows the lowest level of contamination of the species (Table 4). The slight declining trend with depth in most species (Na^+ shows a slight positive trend), is not likely of climatic origin because it would be unlikely to affect particular sample positions in the borehole systemically. The data suggest that the contamination source for sample 1 is not significantly cleaned by repeated use.

Comparison with ice cores

To assess whether the chemical data from RAID samples can be used to make climatic interpretations, the data were compared to the nearest ice cores. For SI:RAID, the data were compared to the 20 m firn core drilled on Sherman Island during the same field season (Fig. 10) (Tetzner and others, 2022). For LDC:RAID2, the data were compared to similarly aged sections from the EDC ice core (Fig. 11). The ice core data are shown on their original depth resolutions and therefore show more variability than the RAID data due to their higher depth resolution. The LDC data are compared by age section due to the varying mean concentrations in the different depths of the core.

The SI:RAID data show very good overlap with the ice core data. The overall levels (Table 5) are very similar. The ion with the largest percentage difference in mean values, Ca^{2+}, has higher values in SI:RAID, likely a result of just three short (~1 m) sections of higher concentrations, seen in Figure 12.

All LDC anion data are above detection limits (Table S1), however for the cation data, some measured values fall below detection limits, due to the low concentration of impurities on the East Antarctic plateau and the inability of standard IC procedures to resolve such concentrations. This is particularly problematic for the Holocene measurements, as shown in Figure 11. All measured samples are shown in Figure 11, to demonstrate this variation in concentrations and the impact on interpretation. Further analysis uses data in which concentrations below the LoB are changed to the LoB. At LDC, there is significant overlap in the data for all ions with EDC in the transition. While the medians of LDC show some variation with respect to EDC, both higher and lower depending on the ion, the magnitude of the inter-quartile range (IQR) is very similar for all ions. In the transition, overall concentrations of all ions are higher at both sites, but most notably for Cl^-, Na^+ and Ca^{2+}, and this well-documented feature is also clear in the LDC:RAID ice chippings. Looking at the more recent sections for these ions, there is a larger difference (less box-plot overlap) between the sites. This is reflective of the lower concentrations in general, which are close to and sometimes below the detection limits for Na^+ (10 µg L^{-1}), Mg^{2+} (3 µg L^{-1}) and Ca^{2+} (5 µg L^{-1}). The MSA^- and SO_4^{2-} data are particularly convincing, with very good overlap of all box-plot parameters during all age sections and the most similar mean values (Table 6).

The similarity in overall concentration and variability extends to the SI data compared on a depth scale, particularly in the top

https://doi.org/10.1017/jog.2022.94 Published online by Cambridge University Press

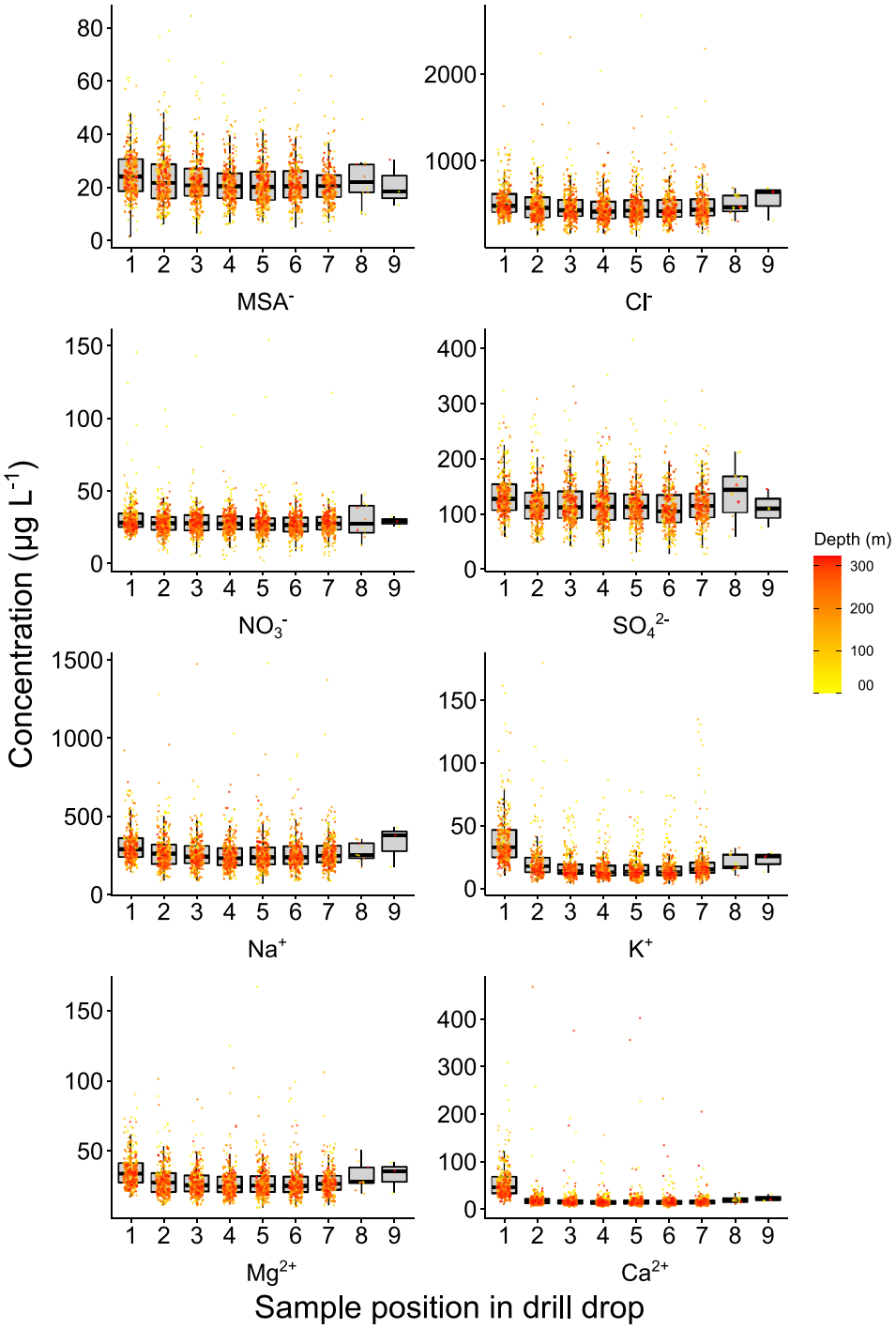

Fig. 7. Major ion chemistry in the Sherman Island RAID samples by position in the drop of each drill. Bold horizontal line shows the median, box shows inter-quartile range (IQR), vertical lines show 1.5 × IQR and scattered dots show every data point with those above or below the vertical lines considered outliers.

Table 4. Percentage increase in the concentrations of SI:RAID samples in the first sample of each drill drop relative to the mean of the remaining samples

Ion	Samples 2–9 µg L^{-1}	Sample 1 µg L^{-1}	Increase in sample 1 %	Difference in means, $t(p)$
MSA^-	22.1	25.4	14.6	5.13 (<0.05)
Cl^-	480.9	544.8	13.3	4.40 (<0.05)
NO_3^-	28.2	31.8	12.5	3.98 (<0.05)
SO_4^{2-}	118.5	136.2	14.9	6.08 (<0.05)
Na^+	268.8	319.2	18.8	6.02 (<0.05)
K^+	18.3	39.3	114.5	14.36 (<0.05)
Mg^{2+}	28.5	36.2	27.1	9.01 (<0.05)
Ca^{2+}	19.0	56.8	199.8	14.51 (<0.05)

13 m. Figure 12 shows the similarity of features including clearly visible annual layers, particularly in the MSA^- and SO_4^{2-} records. A large peak in multiple ions at ~2 m depth is identified in both the chippings and the core. Increasing with depth beyond 13 m, there is less agreement in the placement of peaks and troughs in the record which are of seasonal origin. The annual layering and thinning of snow and ice at sites 2 km apart is not likely to be identical and discrepancies will be propagated with increasing depth in the core, so some displacement of features between the records is to be expected. This result does however, demonstrate that chemical data from RAID chippings is of sufficient quality to observe peaks and troughs, including seasonal signals, faithfully. These data also highlight the importance of sampling

https://doi.org/10.1017/jog.2022.94 Published online by Cambridge University Press

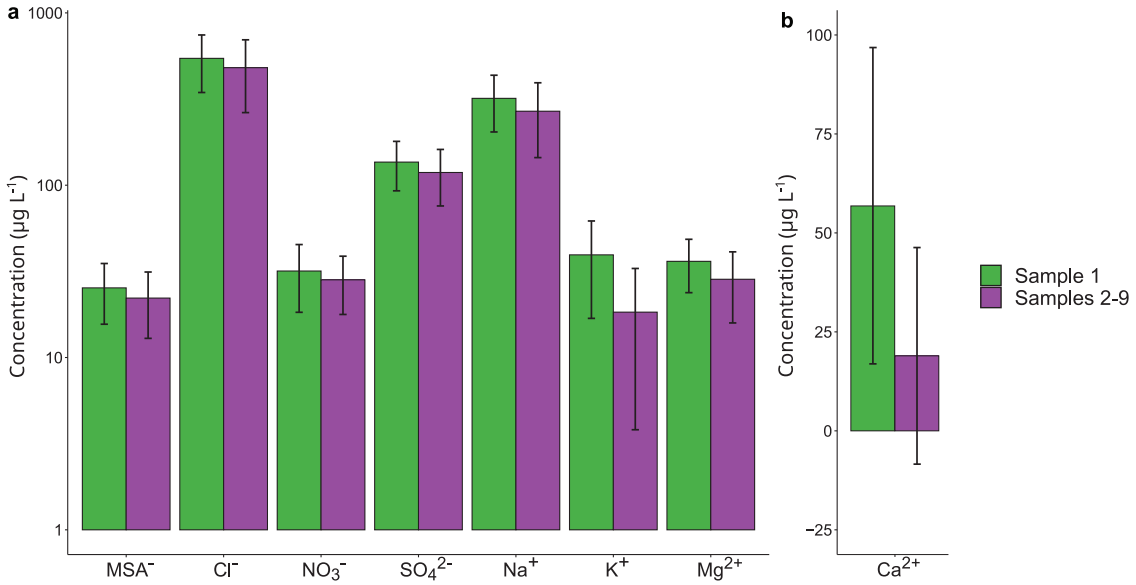

Fig. 8. A comparison of the mean of the first sample in each drill drop of SI:RAID samples, with the mean of the remaining samples (2–9). Error bars show the SD. Panel A shows MSA^-, Cl^-, NO_3^-, SO_4^{2-}, Na^+, K^+ and Mg^{2+}. Panel B shows Ca^{2+} on a separate *y*-axis scale for clearer visualisation.

resolution in identifying seasonal variations, which is a limiting factor of RAID drilling.

As a final demonstration that the RAID chippings' data can assess the geochemical relationships in ice, the relationship between Cl^- and Na^+ concentrations at Sherman Island is shown in Figure 13 and at Dome C in Figure 14. The direct positive relationship ($r^2 = 0.97$ for SI:RAID and 0.99 for SI:Core) between Cl^- and Na^+ at Sherman Island is clear and a simple linear model fitted to the data emphasises the ratio of 1.7, close to that of the Cl^- weight ratio to Na^+ in sea water (1.795, Chesselet and others, 1972; Bertler and others, 2005). The relationship at LDC is more complex and thus a single model was not fitted. However, the different sections clearly demonstrate differing relationships between the ions with an overall positive relationship (Fig. 14). The transition period shows the highest concentrations at both sites, and this is the time period of most confidence in the data based on detection limits (Fig. 11). Although the overall pattern when comparing the relative slopes of each time period is similar at both sites, there are differences in the other time periods, such as a steeper slope in the Late Holocene relative to the Early Holocene and ACR at LDC compared with EDC, which shows the steepest slope for the ACR (not including Transition). These differences could be due to: different ratios of impurities reaching LDC compared with EDC, with the sites being located 40 km apart; differences in chemical reactions during transport; or differences in chemical reaction after deposition onto the ice sheet (Legrand and Delmas, 1988).

Water isotopes

The δ^2H records of the SI:RAID and SI:Core samples are shown in Figure 15. A filtered SI:Core record is shown. The depth-scale plot (panel A) shows that when the SI:Core (SD 15.0) is interpolated to the RAID resolution, with a 3-point centred moving average applied, the SD is reduced to 10.9, lower than an SD of 12.6 for the SI:RAID samples. The pattern of variability is broadly the same within both records and like with the chemical ion records this similarity is strongest in the upper 12–15 m. For example, the prominent troughs at ~1.5 and 4 m, followed by a section of higher values and lower variation between ~5 and 7.5 m are visible in both lines. Annual cycles are visible throughout the 20 m of the RAID samples as well as in the core. Smaller, sub-annual features also vary comparably, for example the broad shoulder peak at ~6 m and the double peak at 12.5 m with a rapid drop in between. Differences between the records include some sections of opposing variability, for example a trough in the RAID data at 15 m coincides with a peak in the core, and the overall mean of the RAID values is slightly lower (Table 7). This is highlighted in panel B, where it is clear that the correlation between the two records is most significant for the 0–12.5 m range. Neither record shows an overall trend (slopes of data in Fig. 15 SI:Core and SI:RAID are 0.42 and 0.09 respectively) therefore the overall variance of the records could be used to investigate the potential smoothing effects of RAID drilling and sampling. A table of the variance statistics is shown in Table 7 and discussed below.

The slopes of the water lines of the SI:RAID and LDC:RAID2 samples (Supplementary Figs S3 and S4) are consistent with those of the global meteoric water line (8.02, Craig, 1961). This result demonstrates that the RAID samples can be reliably measured for water isotopic ratios. The signal is as climatologically meaningful as in the equivalent resolution of traditional ice core samples. This reliability is clearly seen for LDC:RAID2 in Figure 16 where the long-term climate features (e.g. glacial termination, ACR) are all visible. Assessing the comparability of higher frequency changes would require an established age scale for the LDC:RAID2 record. The absolute difference in deuterium ratio between the two sites is an interesting result which is the subject of discussion in a separate paper currently in preparation, investigating the water isotope records of multiple ice cores near Dome C.

There is no reason to expect any systemic contamination of water isotope composition equivalent to that seen in the IC data in Figures 7 and 9. Figure S5, showing the water isotope data presented by drop position, confirms this.

Discussion

Similarity to ice core records

It should be noted that neither of the ice cores used to assess the RAID records are from precisely the same location as the RAID drill sites. Some differences, due to stratigraphic noise and

https://doi.org/10.1017/jog.2022.94 Published online by Cambridge University Press

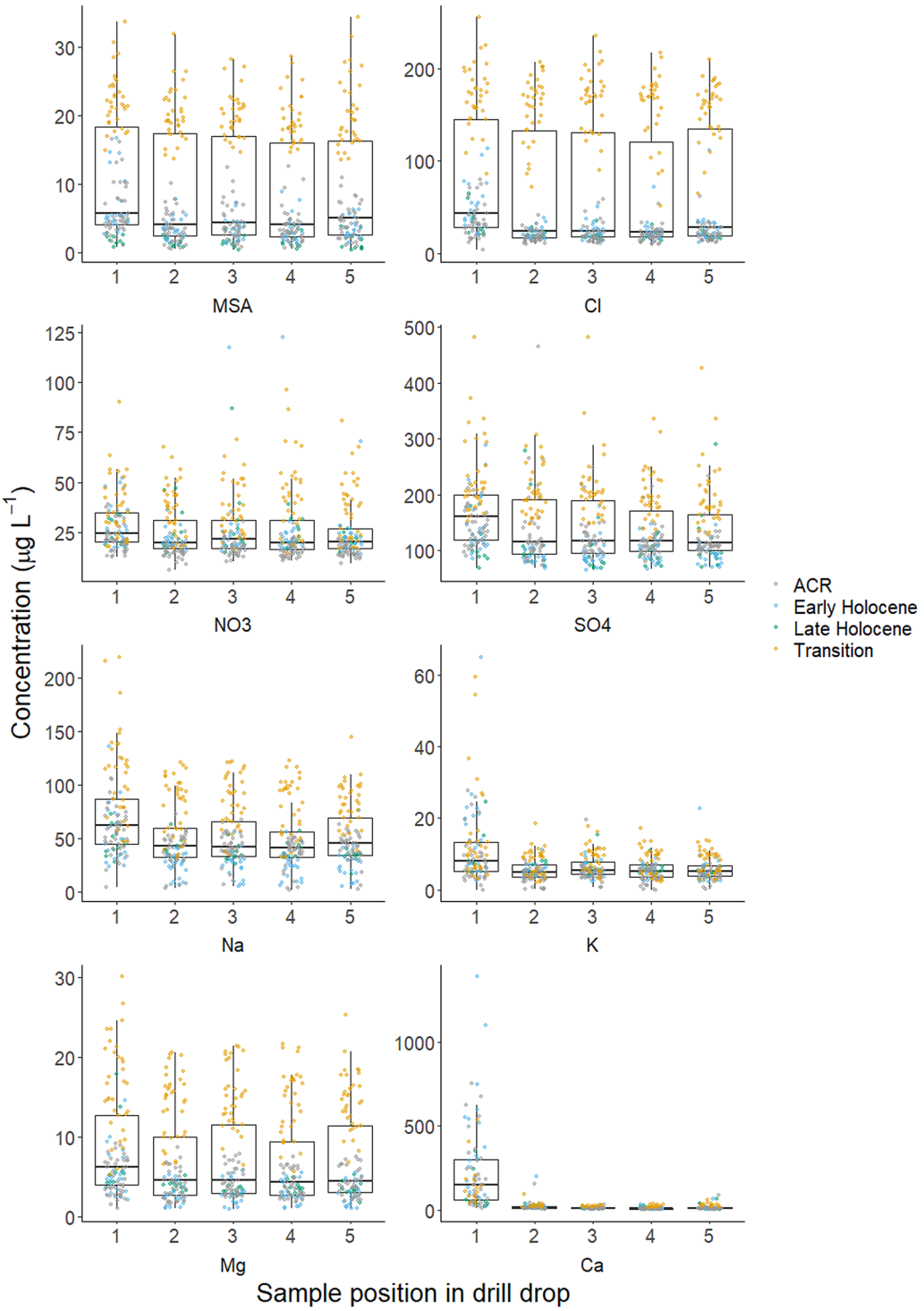

Fig. 9. Major ion chemistry in the LDC:RAID2 samples by position in the drop of each drill, with coloured points showing the section of samples analysed: Early and Late Holocene, Antarctic Cold Reversal and Glacial Transition. Bold horizontal line shows the median, box shows IQR, vertical lines show 1.5 × IQR and scattered dots show every data point, with those above or below the vertical lines considered outliers. Note: for clarity and to enable easier viewing of the boxes of drops 2 to 5, extreme outliers in the data were removed for this plot, values of NO_3^- over 200 μg L^{-1}, K^+ over 75 μg L^{-1}, Na^+ over 300 μg L^{-1}, Cl^- over 300 μg L^{-1} and MSA^- over 40 μg L^{-1}, a total of five individual samples. These data were considered in statistics tables and remaining analyses.

potentially slightly different climatological conditions, are to be expected, however the overall pattern of variability should be similar. The two locations (Dome C and Sherman Island) are geographically very different, illustrating the ability of RAID sampling to capture different aspects of climate variability. Sherman Island is a coastal West Antarctic site with a relatively high accumulation rate of 58.3 cm w.e. and a strong marine influence (Tetzner and others, 2022). LDC is on the East Antarctic plateau with low accumulation of ~2 cm w.e., a typically continental chemical signature and low water isotope values (Bigler and others, 2006; Masson-Delmotte and others, 2008; Genthon and others, 2016; Parrenin and others, 2017; Cavitte and others, 2018). The aim here is to assess the ability of the RAID samples to display the two very different chemical and water isotopic climate signals. It is unsurprising that the RAID water isotope records show good similarity with nearby cores in terms of

https://doi.org/10.1017/jog.2022.94 Published online by Cambridge University Press

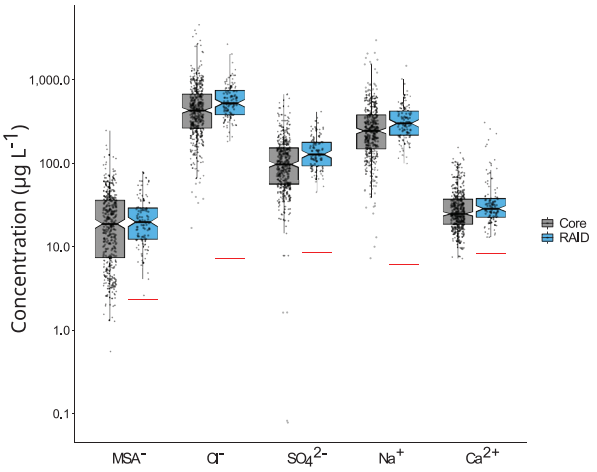

Fig. 10. Major chemistry content in the top 20 m of SI:RAID samples with the contaminated Ca^{2+} data removed, compared with available data from the 20 m SI:Core, by ion. Bold horizontal line shows the median, box shows IQR, vertical lines show 1.5 × IQR, box notches show median $\pm 1.57(\mathrm{IQR}/\sqrt{(n)})$ and scattered dots show every data point, with those above or below the vertical lines considered outliers. Red lines show LoB for each ion.

The overall similarity of the chemical data at both sites with their respective comparison cores is very good, discarding the first RAID sample of each drop. Ice cores are typically dated using a combination of techniques including annual layer counting, volcanic synchronisation and methane synchronisation, among others (e.g. Buizert and others, 2015; Sigl and others, 2016; Severi and others, 2022). The small, broken ice chippings drilled by the RAID make gas measurements implausible. Here, we show that seasonal cycles of chemical and water isotopic data are visible and could be used for annual layer counting of shallower sections. IC results, particularly the convincing similarity of SO_4^{2-} (Figs 10 and 11), suggest that dating by volcanic synchronisation of SO_4^{2-} peaks tied to dated cores could be possible if peaks are identifiable once the resolution becomes lessened by thinning in addition to low-resolution sampling (e.g. Udisti and others, 2004). If the sampling resolution and accumulation rate, which is site specific, are sufficient, the width of SO_4^{2-} peaks taking place over more than one sample could be adequate for identifying known volcanic events. This is especially likely for recent years in the shallower, less thinned portion of the ice record, for example the 1815 Tambora eruption which has been identified in multiple Antarctic ice cores (Sigl and others, 2014).

their variability at both sites; there is no reason that the drilling method should interfere with the isotopic composition of the ice. The data comparisons here clearly validate this original purpose of the BAS RAID. Only the sampling resolution limits the ability of RAID data to pick up all of the potential water isotope variability recorded in the ice.

Mixing of ice and attenuation of signal

A simple way to determine potential attenuation of the isotopic signal caused by mixing of chippings inside the drill barrel and sampling tube is to compare the variance and SD of the records with similarly resolved ice cores. The SI and EDC comparison cores are at higher and lower resolution than the RAID chippings,

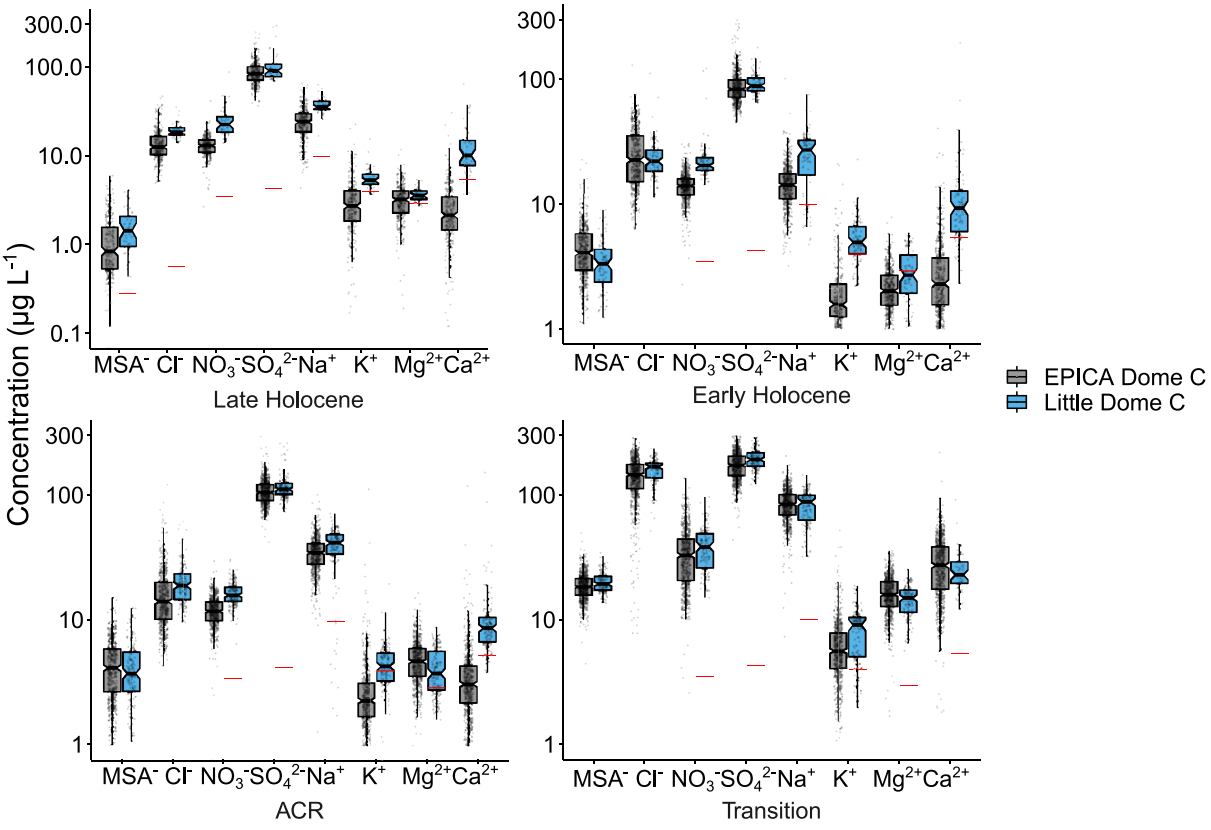

Fig. 11. Major chemistry content in the LDC:RAID2 samples with contaminated data removed, compared with the same aged sections in the EDC core, by ion (*x*-axis) and section (panels). Bold horizontal line shows the median, box shows IQR, vertical lines show 1.5 × IQR, box notches show median $\pm 1.57(\mathrm{IQR}/\sqrt{(n)})$ and scattered dots show every data point, with those above or below the vertical lines considered outliers. With the exception of the Late Holocene panel which extends the *y*-axis to 0.1 to demonstrate the LoBs for MSA^- and Cl^-, the *y* limit is cut-off at 1 (rather than 0) to enable easier viewing of the relevant data, justified on the basis that 1 µg L^{-1} is below the detection limit of all remaining LDC:RAID measurements. Red lines show LoB for each ion.

https://doi.org/10.1017/jog.2022.94 Published online by Cambridge University Press

Table 5. Summary statistics of the top 20 m of the SI:RAID and available SI ice core chemistry data, with the contaminated Ca^{2+} data removed

	SI:RAID					SI-Core				
Ion	Mean μg L^{-1}	Median μg L^{-1}	SD	25th % μg L^{-1}	75th % μg L^{-1}	Mean μg L^{-1}	Median μg L^{-1}	SD	25th % μg L^{-1}	75th % μg L^{-1}
MSA^-	24.42	19.93	16.85	12.32	29.44	25.89	18.90	26.03	7.41	36.28
Cl^-	615.18	526.68	350.14	383.63	750.96	551.33	433.43	507.25	265.81	677.34
SO_4^{2-}	146.85	129.41	69.23	93.62	180.88	124.32	98.50	100.26	55.58	155.09
Na^+	345.17	301.34	192.93	216.98	423.65	318.64	244.75	304.90	149.54	381.44
Ca^{2+}	43.81	28.79	48.01	22.63	38.21	32.01	24.93	21.40	18.65	37.55

respectively. This difference presents an interesting opportunity to perform the variance reduction two ways -- one way reducing LDC:RAID2 variance to match the EDC core, and another reducing SI:Core variance to match the SI:RAID, as described below.

To simulate the reduction in variability of a 5 cm record to a 17 cm record, it was necessary to linearly interpolate the SI:Core to the same resolution as the RAID, and perform a 3-point smoothing moving average. Smoothing or interpolating alone were insufficient to reduce the SD and variance to the SI:RAID values. This calculation resulted in the core having an SD and variance less than the RAID (of 14.2 and 28.4% respectively), which would not be expected if we assume that at least some mixing of chippings takes place. Some differences are to be expected in the short-term (20 year) isotope variations of two high-resolution ice cores situated 2.7 km apart (Fisher and others, 1985; Karlof and others, 2006; Laepple and others, 2017). In general though, this result implies that there is minimal, if any, smoothing as a result of chippings getting mixed.

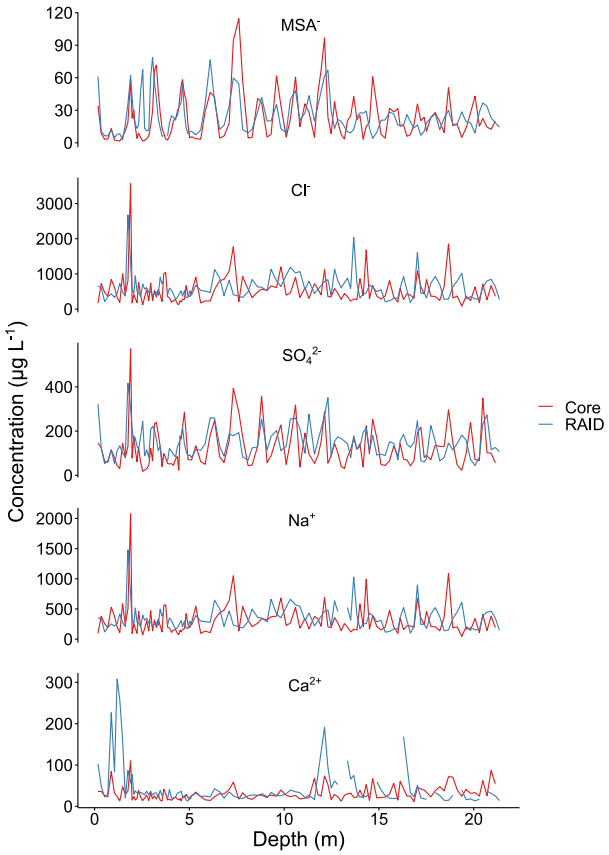

Fig. 12. Major ions in the Sherman Island ice core (red) interpolated to the depth resolution of the RAID samples, and top 20 m of RAID chippings (blue) after contaminated data removed, presented on a depth scale.

The 27 cm LDC:RAID2 deuterium data had a full dataset SD of 15.5, compared with the 55 cm EDC data SD of 13.8. Smoothing the LDC data by a 2-point moving average reduced the SD to 14.7, which was further reduced to 14.2 with interpolation to the reduced resolution of the EDC record. This reduction in variance results in the SDs differing by only 1.4%, with the data still more variable in the RAID chippings than in the core. It is possible that the isotopic variations at LDC are greater in magnitude than at EDC. However, it is not likely that this would be visible in the isotope data considering the lower accumulation rate at LDC, shown by the shallower depths of the glacial–Holocene transition apparent in Figure 16. It is also important to consider that the SD of these records is in part due to the magnitude of this transition. However, without an appropriate age scale for the LDC record, it is difficult to compare exactly the same time periods to further investigate this difference.

There is a greater difference in the variability of the records at Sherman Island than at Dome C. This may be expected given the higher accumulation rate and shorter timescales being investigated. The RAID and core data show similar variance once they are adjusted for different resolutions (Table 7), and also show very similar climatic changes (Figs 12, 15 and 16). These conclusions are applicable to two very climatologically different sites. The findings from both sites suggests that the overall impact of mixing inside the drill barrel and sampling tube, as well as shifting of ice chippings during sampling, has a limited impact on attenuating or dampening the variability in the resultant isotope record. This finding is in agreement with one other study using ^{10}Be measurements from the LDC:RAID2 chippings, which found a negligible effect of mixing in the RAID on the ^{10}Be signal (Nguyen and others, 2021). Further investigation using higher resolution RAID chippings would make this impact more quantifiable.

This work aims to define an upper limit of the effective attenuation of the signal caused by mixing of chippings in the drill barrel and during sampling. However, given that both RAID sites are not at the same locations as the comparison cores, any observed differences in the signals could also be due to differences in stratigraphy, caused by wind scouring and other post-depositional effects, as well as slightly different climate signals and contents of precipitation. The analysis of the stable water isotopes presented in Figures 15 and 16 and Table 7 demonstrates minimal impact of RAID drilling and sampling on signal variability. As shown from Figure 12 this result is applicable to the chemical ion data, where differences are likely due to RAID sampling resolution and stratigraphic differences, rather than mixing-induced attenuation of the signal.

Chemical contamination

The results in Figures 7 and 9 show a clear contamination signal, which we can confidently conclude is present only in the first sample of each drop of the drill. The source of the contamination therefore likely resides in the top section of hollow barrel where

https://doi.org/10.1017/jog.2022.94 Published online by Cambridge University Press

Table 6. Summary statistics of the LDC:RAID2 and EDC ice core chemistry data, with the contaminated K^+ and Ca^{2+} data removed

	LDC:RAID2					EDC-Core				
Ion	Mean μg L^{-1}	Median μg L^{-1}	SD	25th % μg L^{-1}	75th % μg L^{-1}	Mean μg L^{-1}	Median μg L^{-1}	SD	25th % μg L^{-1}	75th % μg L^{-1}
MSA^-	8.81	4.39	8.22	2.57	16.59	9.01	5.46	8.01	2.73	16.12
Cl^-	65.17	24.02	67.23	17.86	132.62	62.70	24.56	66.71	13.42	117.97
NO_3^-	26.27	20.38	15.49	17.05	30.79	21.18	14.81	18.93	11.71	23.48
SO_4^{2-}	140.51	116.41	62.37	96.09	177.53	130.19	111.96	69.81	85.08	159.73
Na^+	50.19	42.35	28.60	32.55	62.64	46.39	34.81	33.98	18.35	72.14
K^+	5.88	5.13	3.24	3.81	7.15	3.88	2.60	4.75	1.33	5.15
Mg^{2+}	7.11	4.56	5.66	2.90	10.89	8.01	4.71	7.24	2.54	13.13
Ca^{2+}	15.45	10.55	16.77	7.59	18.07	12.35	3.89	16.27	1.90	19.51

chippings are contained. Furthermore, Figure 6 suggests that the longer drill barrel contains a source of the contaminants, but that this is not present in the shorter barrel. Chemical data for this transition between barrels are available only for the SI:RAID samples, not for LDC. The only difference between the barrels is their length (4.48 and 1.47 m) and the presence in the longer barrel of a plastic – polyoxymethylene, $(CH_2O)_n$ – bearing around the middle of the long spiral, shown in Figure 17. Finally, the contamination is consistent throughout the SI:RAID records (Supplementary Fig. S2), implying that the contamination source(s) reside within the drill itself. Otherwise, a depletion of the contamination amplitude would likely be seen with depth.

To explain the contamination, we must explain several observations: first that only the top sample is contaminated, second that the contamination must be consistently produced or present during every drop of the drill and third that a dominant source of cation contamination (most notably Ca^{2+} and K^+) must be present. Addressing the first point, simple contact with any part of the drill (the barrel, cutters, spiral auger, etc.) or sampling tube can be ruled out because this would result contamination of all samples, not just the top-most sample. One theory is that the plastic bearing is the contamination source. We theorised that when empty and travelling down the borehole, the wobbling or rattling of the barrel or the spiral inside the barrel produces 'dust' as a result of wearing. Once stationary and filled with chippings from drilling, this rattling stops and no more dust is produced. As drilling progresses and the chippings rise up inside the barrel, the top-most (shallowest) chippings rise past the bearing where dust has been produced, and carry it up to the top of the barrel, essentially cleaning out the barrel of contamination for the deeper samples. This mechanism explains the first two observations, however, there is no obvious source of the cation contamination observed that would not also be present in the deeper samples which also touch the bearing.

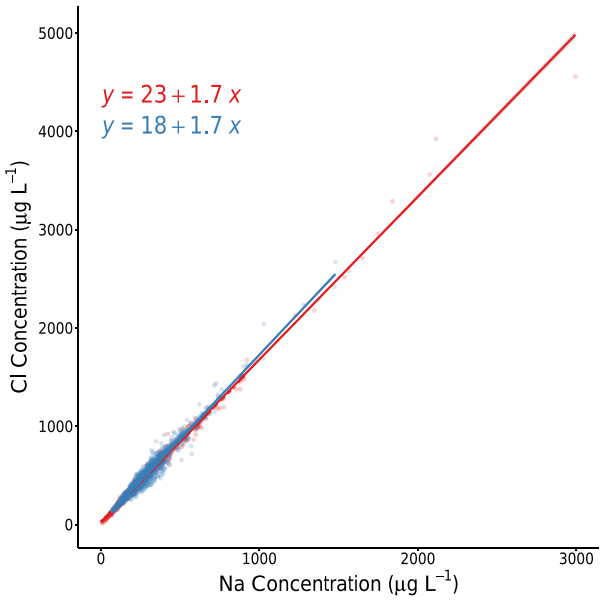

Fig. 13. Cl^- and Na^+ in the Sherman Island RAID samples (blue) and Sherman Island ice core (red).

The precise contamination source and mechanism is still an open question. It is likely that the source of the contamination is in the top of the drill barrel. Regarding the specific cation contamination observed, there is no obvious source from the drill materials themselves, which are primarily composed of varying grades of steel, with some plastic e.g. the xylan coating of the spiral. There is no reasonable or obvious consistently available external source of dust which would only be picked up in the top sample. It could be that dust inside the drill barrel which has always been there is contaminating the sample. However, it would seem reasonable to expect the magnitude of this source to deteriorate over time, which does not appear to be the case. Suggestions for this problem are discussed below.

Future considerations

The results of this study show that the water isotope and chemistry data obtained from RAID-drilled ice are meaningful and of good quality, with the exception of the contamination in certain species in the first sample of each drill drop. Identifying the contamination source and implementing a solution would maximise the use of the RAID.

One investigation could be to perform chemical tests on the length of the barrel. This method might provide more information about the location of the contamination source. Before its next use, the drill should be rinsed with MQ water. Rinsing should result in the inside of the drill barrel being chemically clean and rinsed of dust. The drill should then be sealed until it is used in the field. If after these measures, the periodic contamination still appears, this would suggest that the contamination is being produced inside the drill as a result of its operation, possibly by one of the mechanisms described above. If, as a result of the chemical testing described above, this is believed to come from the top of the drill barrel as we suspect, then to alleviate sample contamination, a solution could be to insert a 'spacer' into the top of the barrel, at the top of the spiral and below the attachment and release mechanism (Fig. 1). This spacer could effectively catch any of the contaminating material coming from the top of the barrel and would be a low cost and minimal solution which should not impact on the engineering or workings of the drill itself.

It should be stressed that while the chemical data are useful without these considerations or drill modifications, the data should be used with caution. Sensible precautions are to use smoothed, or binned averages of the data to investigate longer

https://doi.org/10.1017/jog.2022.94 Published online by Cambridge University Press

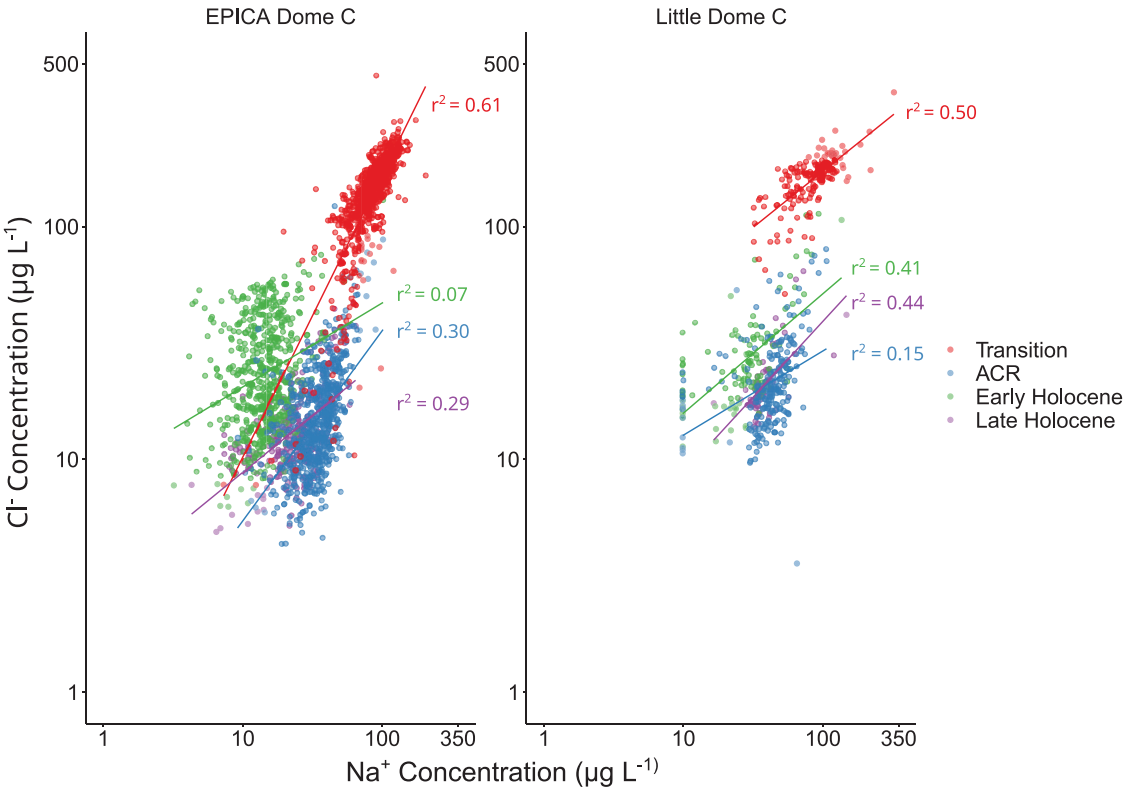

Fig. 14. Cl^- and Na^+ in the LDC RAID samples, coloured by age section.

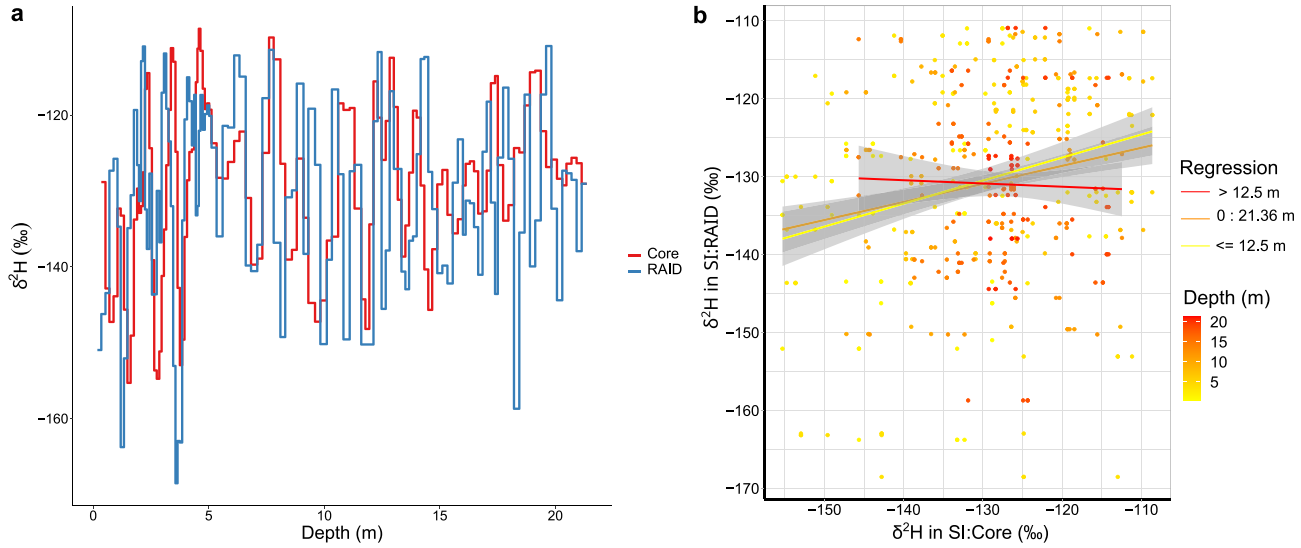

Fig. 15. (A) δ^2H (‰) on a depth scale from the SI:RAID samples (blue), and SI:Core interpolated onto RAID sample resolution and with a 3-point centred-moving average (red). (B) Scatter plot of the SI:RAID (*y*-axis) against the SI:Core (*a*-axis) δ^2H ratio (‰) coloured by depth (colour scale), with regression lines for the full depth range (orange), 0–12.5 m (yellow) and 12.5–21 m (red).

Table 7. Statistics of 21 m δ^2H ratio (‰) records from the SI:RAID samples and SI:Core samples shown as raw data, and smoothed with a 2-point moving average and interpolated on to SI:RAID resolution

Core type	Mean ‰	SD	Variance
Core – original	−129.4	15.03	225.84
Core – interpolated and smoothed	−129.3	10.94	119.58
RAID – original	−130.8	12.61	159.09

term changes at the sites drilled, rather than the data in their analysis resolution. Furthermore the data could be very useful for dating and the comparison and validation of nearby ice core data, but less so for detailed and high spatial resolution palaeoclimate interpretation of the specific site.

Without the issue of contamination, the main factor limiting interpretation is the sampling resolution. This is within the control of the drillers in the field but is limited by logistical

https://doi.org/10.1017/jog.2022.94 Published online by Cambridge University Press

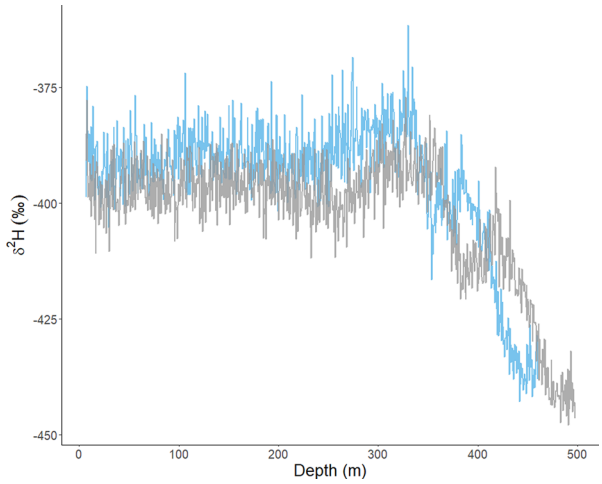

Fig. 16. EDC and LDC:RAID2 deuterium records on a depth scale, with LDC (blue – average 27 cm resolution) smoothed by a 2-point centred moving average to reduce the variability to a level similar to EDC and interpolated onto the same depth points as the EDC data (grey – 55 cm resolution). The shift in the depths of climatic features such as the deglaciation and Antarctic Cold Reversal is due to the lower accumulation rate at the LDC site.

capabilities, sample storage and the desire to keep equipment and transport minimal, which is a significant advantage of RAID drilling in the first place. The specific sampling regime should be determined individually and should be informed by known site information including accumulation rate and the specific project aims, while bearing in mind the potential use of drilled samples for future unknown projects. If deemed necessary, a taller and thinner sampling tube using the same mechanism could be designed, with a larger number of smaller sampling windows to enable higher resolution sampling while minimising mixing. A built in funnel could be designed into the sampling tube to reduce the number of pieces of equipment and potential sources of contamination. It would be very interesting, with the next use of the RAID, to drill multiple shallow cores adjacent to the RAID on the order of a few metres depth and within a few metres of horizontal distance to the RAID borehole, and sample the RAID chippings at high resolution (e.g. ~5 cm). These samples would enable a thorough analysis of the effects of mixing on attenuation of the records.

Conclusions

The RAID was originally designed for obtaining low-resolution isotope measurements, primarily for assessing prospective sites for traditional deep drilling projects. More data are being obtained from RAID chippings than was initially proposed, specifically chemistry and measurements of ^{10}Be, and further analyses may well be possible in the future (Nguyen and others, 2021). Here, we show that the isotope signals derived from RAID chippings are accurate and climatologically meaningful. The original aims of the drill have been satisfied and the drill can confidently be used in the future. Furthermore, we have presented major ion chemistry from the RAID chippings, which although limited in interpretation by a consistent contamination source, is still meaningful and could be used for dating and climate interpretations. The chemical contamination source should be investigated further and a suitable mitigation strategy implemented, to maximise the potential of future RAID samples. Further considerations regarding the sampling resolution and storage conditions should be decided based on future project requirements. The results from this new drilling technique are promising and widen the potential use of the RAID from prospective ice core assessment, to additional rapid replicate coring alongside existing large-scale deep ice coring projects such as Beyond EPICA and Hercules Dome (Jacobel and others, 2005; Schiermeier, 2016; Tollefson, 2019). The RAID could become a useful tool for many ice coring projects, generating additional data with lower logistics and personnel demands, representing a very promising addition to the ice core science community.

Supplementary material. The supplementary material for this article can be found at https://doi.org/10.1017/jog.2022.94.

Acknowledgements. The authors thank Shaun Miller and Jack Humby for assistance with lab analyses. The authors also thank BAS field guides Sarah Crowsley and Tom King for their help and positivity in the field. This project has received funding from the European Research Council under the Horizon 2020 research and innovation programme (grant agreement No. 742224, WACSWAIN). This material reflects only the author's views and the Commission is not liable for any use that may be made of the information contained therein.

References

Alemany O and 21 others (2014) The SUBGLACIOR drilling probe: concept and design. *Annals of Glaciology* **55**(68), 233–242. doi:10.3189/2014AoG68A026

Armbruster DA and Pry T (2008) Limit of blank, limit of detection and limit of quantitation. *The Clinical Biochemist Reviews* **29**(1), S49–S52.

Bertler N and 47 others (2005) Snow chemistry across Antarctica. *Annals of Glaciology* **41**, 167–179. doi:10.3189/172756405781813320

Bigler M, Röthlisberger R, Lambert F, Stocker TF and Wagenbach D (2006) Aerosol deposited in East Antarctica over the Last Glacial cycle: detailed apportionment of continental and sea-salt contributions. *Journal of Geophysical Research: Atmospheres* **111**(D8), D08205. doi:10.1029/2005JD006469

Buizert C and 16 others (2015) The WAIS Divide deep ice core WD2014 chronology – part 1: methane synchronization (68–31 ka BP) and the Gas Age–Ice Age difference. *Climate of the Past* **11**(2), 153–173. doi:10.5194/cp-11-153-2015

Cavitte MGP and 7 others (2018) Accumulation patterns around Dome C, East Antarctica, in the last 73 kyr. *The Cryosphere* **12**(4), 1401–1414. doi:10.5194/tc-12-1401-2018

Chesselet R, Morelli J and Buat-Menard P (1972) Variations in ionic ratios between reference sea water and marine aerosols. *Journal of Geophysical Research (1896–1977)* **77**(27), 5116–5131. eprint https://onlinelibrary.wiley.com/doi/pdf/10.1029/JC077i027p05116. doi:10.1029/JC077i027p05116

Craig H (1961) Standard for reporting concentrations of deuterium and oxygen-18 in natural waters. *Science* **133**(3467), 1833–1834. doi:10.1126/science.133.3467.1833

EPICA community members (2004) Eight Glacial cycles from an Antarctic ice core. *Nature* **429**(6992), 623–628. doi:10.1038/nature02599

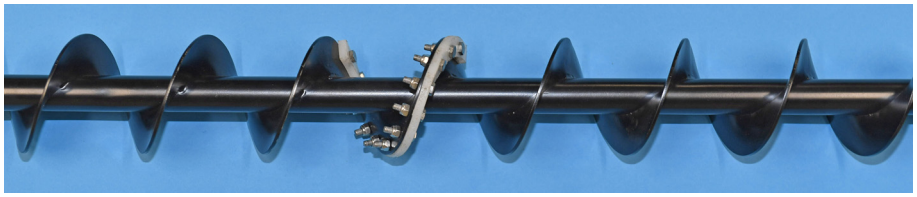

Fig. 17. Plastic (Delrin) bearing around the centre of the longer drill spiral.

Fischer H and 29 others (2013) Where to find 1.5 million yr old ice for the IPICS Oldest-Ice ice core. *Climate of the Past* **9**(6), 2489–2505. doi:10.5194/cp-9-2489-2013

Fisher DA, Reeh N and Clausen H (1985) Stratigraphic noise in time series derived from ice cores. *Annals of Glaciology* **7**, 76–83. doi:10.3189/S0260305500005942

Genthon C, Six D, Scarchilli C, Ciardini V and Frezzotti M (2016) Meteorological and snow accumulation gradients across Dome C, East Antarctic plateau. *International Journal of Climatology* **36**(1), 455–466. doi:10.1002/joc.4362

Goodge JW and Severinghaus JP (2016) Rapid access ice drill: a new tool for exploration of the deep Antarctic ice sheets and subglacial geology. *Journal of Glaciology* **62**(236), 1049–1064. doi:10.1017/jog.2016.97

Jacobel RW, Welch BC, Steig EJ and Schneider DP (2005) Glaciological and climatic significance of Hercules Dome, Antarctica: an optimal site for deep ice core drilling. *Journal of Geophysical Research: Earth Surface* **110**. doi:10.1029/2004JF000188

Karlof L, Winebrenner DP and Percival DB (2006) How representative is a time series derived from a firn core? A study at a low-accumulation site on the Antarctic plateau. *Journal of Geophysical Research: Earth Surface* **111** (F4), F04001. wOS:000241298500001. doi:10.1029/2006JF000552

Laepple T, Münch T and Dolman A (2017) Inferring past climate variations from proxies: separating climate and non-climate variability. *Past Global Changes Magazine* **25**(3), 140–141. doi:10.22498/pages.25.3.140

Legrand MR and Delmas RJ (1988) Formation of HCl in the Antarctic atmosphere. *Journal of Geophysical Research: Atmospheres* **93**, 7153–7168. doi:10.1029/JD093iD06p07153

Lilien DA and 13 others (2021) Brief communication: new radar constraints support presence of ice older than 1.5 Myr at Little Dome C. *The Cryosphere* **15**(4), 1881–1888. doi:10.5194/tc-15-1881-2021

Littot GC and 9 others (2002) Comparison of analytical methods used for measuring major ions in the EPICA Dome C (Antarctica) ice core. *Annals of Glaciology* **35**, 299–305. doi:10.3189/172756402781817022

Masson-Delmotte V and 35 others (2008) A review of Antarctic surface snow isotopic composition: observations, atmospheric circulation, and isotopic modeling. *Journal of Climate* **21**(13), 3359–3387. doi:10.1175/2007JCLI2139.1

Matsuoka K and 21 others (2021) Quantarctica, an integrated mapping environment for Antarctica, the Southern Ocean, and sub-Antarctic islands. *Environmental Modelling & Software* **140**, 105015. doi:10.1016/j.envsoft.2021.105015

Mulvaney R and 8 others (2021) Ice drilling on Skytrain Ice Rise and Sherman Island, Antarctica. *Annals of Glaciology* **62**(85–86), 311–323. doi:10.1017/aog.2021.7

Nguyen L and 8 others (2021) The potential for a continuous ^{10}Be record measured on ice chips from a borehole. *Results in Geochemistry* **5**, 100012. doi:10.1016/j.ringeo.2021.100012

Parrenin F and 11 others (2017) Is there 1.5-million-year-old ice near Dome C, Antarctica?. *The Cryosphere* **11**(6), 2427–2437. doi:10.5194/tc-11-2427-2017

Passalacqua O and 6 others (2018) Brief communication: candidate sites of 1.5 Myr old ice 37 km southwest of the Dome C summit, East Antarctica. *The Cryosphere* **12**(6), 2167–2174. doi:10.5194/tc-12-2167-2018

Rix J, Mulvaney R, Hong J and Ashurst D (2019) Development of the British Antarctic Survey Rapid Access Isotope Drill. *Journal of Glaciology* **65**(250), 288–298. doi:10.1017/jog.2019.9

Schiermeier Q (2016) Speedy Antarctic drills start hunt for Earth's oldest ice. *Nature* **540**(7631), 18–19. number: 7631. doi:10.1038/540018a

Schwander J, Marending S, Stocker TF and Fischer H (2014) RADIX: a minimal-resources rapid-access drilling system. *Annals of Glaciology* **55**(68), 34–38. doi:10.3189/2014AoG68A015

Severi M, Udisti R, Becagli S, Stenni B and Traversi R (2012) Volcanic synchronisation of the EPICA-DC and TALDICE ice cores for the last 42 kyr BP. *Climate of the Past* **8**(2), 509–517. doi:10.5194/cp-8-509-2012

Sigl M and 15 others (2014) Insights from Antarctica on volcanic forcing during the Common Era. *Nature Climate Change* **4**(8), 693–697. doi:10.1038/nclimate2293

Sigl M and 26 others (2016) The WAIS Divide deep ice core WD2014 chronology – part 2: annual-layer counting (0–31 ka BP). *Climate of the Past* **12** (3), 769–786. doi:10.5194/cp-12-769-2016

Stenni B and 14 others (2010) The deuterium excess records of EPICA Dome C and Dronning Maud Land ice cores (East Antarctica). *Quaternary Science Reviews* **29**(1–2), 146–159. doi:10.1016/j.quascirev.2009.10.009

Tetzner DR, Allen CS and Thomas ER (2022) Regional variability of diatoms in ice cores from the Antarctic Peninsula and Ellsworth Land, Antarctica. *The Cryosphere* **16**(3), 779–798. doi:10.5194/tc-16-779-2022

Tollefson J (2019) The hunt for ancient ice that witnessed West Antarctica's collapse. *Nature* **576**(7786), 193–194. bandiera_abtest: a Cg_type: News Number: 7786. doi:10.1038/d41586-019-03793-w

Udisti R and 8 others (2004) Stratigraphic correlations between the European Project for Ice Coring in Antarctica (EPICA) Dome C and Vostok ice cores showing the relative variations of snow accumulation over the past 45 kyr. *Journal of Geophysical Research: Atmospheres* **109**, D08101. doi:10.1029/2003JD004180

Wilhelms F and 8 others (2006) *White paper: Ice Core Drilling Technical Challenges*. Technical report, International Partnerships in Ice Core Sciences, PAGES.

https://doi.org/10.1017/jog.2022.94 Published online by Cambridge University Press